



Effects of Strong Magnetic Fields on Neutron Star Structure

a systematic study of the magnetic field contribution to the neutron star structure

تأثيرات المجال المغناطيسي القوي على بنية

النجم النيوتروني

دراسة منهجية لمساهمة المجال المغناطيسي في بنية النجم النيوتروني

Omar Alfarooq Obidieh

Supervisor: Dr. Hazem AbuSara

February 2020



Effects of Strong Magnetic Fields on Neutron Star Structure

a systematic study of the magnetic field contribution to the neutron star structure

تأثيرات المجال المغناطيسي القوي على بنية

النجم النيوتروني

دراسة منهجية لمساهمة المجال المغناطيسي في بنية النجم النيوتروني

Omar Alfarooq Obidieh

Supervisor: Dr. Hazem AbuSara

This thesis was submitted in partial fulfillment of the requirements for the
Master's Degree in Physics from the Faculty of Graduate Studies at Birzeit
University, Palestine

February 2020

Effects of Strong Magnetic Fields on Neutron Star Structure

a systematic study of the magnetic field contribution to the neutron star structure

تأثيرات المجال المغناطيسي القوي على بنية

النجم النيوتروني

دراسة منهجية لمساهمة المجال المغناطيسي في بنية النجم النيوتروني

Omar Alfarooq Obidieh

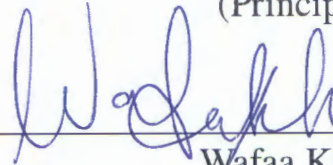
Accepted by the Faculty of Graduate Studies, Birzeit University, in partial
fulfillment of the degree of Master of Physics

Thesis committee:



Hazem AbuSara, Ph.D.

(Principal Advisor)



Wafaa Khater, Ph.D.

(Member)



Isma'el Badran, Ph.D.

(Member)

February 2020

I dedicate this thesis to my loving parents and dear fiancée. ...

Acknowledgements

I want to demonstrate appreciation to my adviser, Dr. Hazem AbuSara, for his continued support throughout this study and related research project. I would also like to thank him for his patience, motivation, and for sharing his tremendous knowledge. Guiding him all the time helped me research and write this thesis. I couldn't have imagined a better master's advisor and mentor.

I also thank my friends, who helped me overcome many difficulties in finding references and programming languages. I also thank my fiancée, who endured busy times throughout the letter's writing and provided support and encouragement for the work to be done to the fullest extent.

Finally, I would like to express my profound gratitude to my loving parents for providing them continuous support and constant encouragement to me throughout my school years and throughout the process of writing this thesis. This advance would not have been possible without them, Thank you.

Abstract

In this study, we are interested in studying a physical model to predict the effect of the strong magnetic field of neutron stars on their structure. This model can help understand the characteristic of matter in conditions different from Earth, where the density of matter and energy is higher, and the magnetic field is stronger. Most of the time, magnetic fields differentiate depending on the central enthalpy in our model; however, to understand how the magnetic field behaves and its relationship with variables, we tested more than one magnetic field form.

Our model consists of an attractive, uncharged material confined to finite relative space and has a magnetic field. The equation of state is built so that the material is denser and depends on strong magnetization properties. Our neutron star structure is determined by many parameters such as enthalpy, material density, and magnetic medium.

We use the "Poisson-like" partial differential equation solution that evolved from Einstein-Maxwell's equation to determine the shape of magnetic field lines, standard magnetic field, and enthalpy and choose the largest magnetic field possible depending on the central bend. We also use the Tolman - Oppenheimer - Volkov like differential equations to find the relationship of mass and pressure with a star's dimensions.

Our results indicate that the central enthalpy significantly controls the

magnetic field and system state and plays a significant role in the magnetic field curvature within the neutron star and the system's energy. The magnetic field also plays an essential role in the neutron star's formation and structure, whether in its radius or the matter/mass distribution and pressure inside it. It significantly affects the change in the distribution of matter inside the star and its concentration in the core, its distribution on several levels, sometimes according to the magnetic field's shape in each case. Especially in more realistic cases, and this applies to the change of pressure, which is also less affected by the change of the magnetic field.

ملخص

في هذه الدراسة، نحن مهتمون بتطوير نموذج فيزيائي للتنبؤ بتأثير المجال المغناطيسي القوي للنجوم النيوترونية على بنيتها. من الممكن أن يكون هذا النموذج مفيداً لفهم خصائص المادة في ظروف مختلفة عن الأرض حيث تكون كثافة المادة والطاقة عاليتين والمجال المغناطيسي قوي جداً. في معظم الأحيان، تمتاز المجالات المغناطيسية اعتماداً على المحتوى الحراري المركزي في نموذجنا ومع ذلك، ولفهم طريقة سلوك المجال المغناطيسي وعلاقته مع المتغيرات قمنا باختبار أكثر من شكل من أشكال المجال المغناطيسي.

يتكون نموذجنا من مادة غير مشحونة متجاذبة محصورة في فضاء نسبي محدود ولديها مجال منغاطيسي. حيث تم بناء معادلة الحالة بحيث تكون المادة أكثر كثافة وتعتمد على خصائص ممغنطة قوية. يتم تحديد بنية النجم النيوتروني الخاص بنا من خلال العديد من العلامات مثل المحتوى الحراري وكثافة المادة والوسط المغناطيسي.

نقوم باستخدام حل المعادلات التفاضلية الجزئية أبواسون الشبيهة والتي تطورت من معادلة أينشتاين ماكسويل لتحديد شكل خطوط المجال المغناطيسي و

المجال المغناطيسي المعياري والمحتوى الحراري، واختيار أكبر مجال مغناطيسي ممكن اعتمادًا على المحتوى الحراري المركزي. كما نستخدم أيضًا معادلات آتولمان - أوبنهايمر - فولكوف الشبيهة التفاضلية لإيجاد علاقة الكتلة والضغط مع أبعاد النجم.

تشير نتائجنا إلى أن المحتوى الحراري المركزية يتحكم في المجال المغناطيسي وحالة النظام بشكل ملحوظ ويلعب دورًا رئيسيًا في انحناءات المجال المغناطيسي داخل النجم النيوتروني وطاقة النظام. كما أن المجال المغناطيسية يلعب دورًا مهمًا في تكوين وبنية النجم النيوتروني سواءً في نصف قطره أو توزيع المادة والضغط في داخله. فهو يؤثر بشكل كبير على توزيع المادة داخل النجم وتمركزها في النواة ويكون توزيعها على عدة طبقات أحيانًا حسب شكل المجال المغناطيسي في كل حالة وخاصةً في الحالات الأكثر واقعية، وهذا ينطبق على تغير الضغط ولكن تأثير تغير المجال المغناطيسي عليه ملحوظ بشكل أقل.

Contents

1	Introduction	15
1.1	A brief overview of neutron Stars	15
1.2	Magnetic field of neutron stars	16
1.3	Types of neutron stars by the magnetic field	18
1.4	Magnetic field and neutron star structure	23
2	Formalism	28
2.1	System of Equations	28
2.1.1	Energy-Momentum Tensor in the presence of a Magnetic Field	28
2.1.2	Electromagnetic equations	30
2.1.3	Energy-momentum tensor and Einstein equations	32
2.1.4	Magnetostatic equilibrium	33
2.1.5	TOV and TOV-like Systems	35
2.2	Numarical Solution	36
2.2.1	Poisson-like Partial Differential Equations Solution	36
2.2.2	TOV-like System Solution	37
3	Neutron Stars: Properties results	39
3.1	Magnetic Field Profile	39

3.2 Structure of Neutron Star	44
4 Conclusions	49
References	51

List of Figures

1.1	The magnetic field structure of a neutron star in a twisted ring formation. ⁵	17
1.2	A graph showing the distribution in the magnetic field B of all radio, XINS, and magnetic pulsars for which \dot{P} was measured. Inner input: Zoom in to $B > 5 \times 10^{12}G$ to better show the distribution of magnets. ⁸	19
1.3	Internal structure of a neutron star. ¹⁶	22
1.4	(a) Pressure (P) vs. energy density (e) relation is plotted at different values of magnetic field.(a*) Same as in the top but for a different range of energy density. (b) Mass-radius relation, relation is plotted at different magnetic field values. (c) Mass-radius relation,relation is plotted at different temperature values. ²⁴	26
1.5	Neutron stars with a purely toroidal field. Portraits show the strength of the magnetic field for a star of mass $M = 1.68 M_{sun}$. From left to right $\gamma = 1, 2, and 4$. The blue line is the stellar surface. ²⁵	27

3.1	Magnetic field lines in the plane (x, z) of $M_G = 3M_\odot$ Neutron star model is equipped with a magnetic field B and a unique EoS table (see EoS of Table) with the difference in the value of the central enthalpy [c^2] 0.01, 0.1, 0.3, 0.5 in a, b, c, d in series. The bold line indicates the surface of the star and the magnetic moment is along the z-axis.	40
3.2	Magnetic field norm rings in the plane (x, z) of $M_G = 3M_\odot$ Neutron star model is equipped with a magnetic field B and a unique EoS table (see EoS of Table) with the difference in the value of the central enthalpy [c^2] 0.01, 0.1, 0.3, 0.5 in a, b, c, d in series. The bold line indicates the surface of the star and the magnetic moment is along the z-axis.	42
3.3	Enthalpy isocontours in the plane $((x, z)$ of $M_G = 3M_\odot$, the solid rings represent positive enthalpy isocontours, dashed rings negative ones (no matter).	43
3.4	Several shapes of the magnetic field norm $b_l(x)$	45
3.5	(left) $\tilde{m} = m/m_{max}$ vs. $x = \bar{r}/r_{mean}$. (right) mass $m(M_{sun}$ vs. radius $r(km)$	46
3.6	(left) $\tilde{p} = p/p_{max}$ vs. $x = \bar{r}/r_{mean}$. (right) pressure $p(10^{47} N/m^2$ vs. radius $r(km)$	47

List of Tables

1.1 Classes and sub-classes of neutron saters by spin period P_s .¹⁰ 18

Chapter 1: Introduction

1.1 A brief overview of neutron Stars

Prediction of neutron stars began shortly after discovering neutrons, where it was found in 1932 by Sir James Chadwick through his study of the emissions of irradiated beryllium. After less than two years, Baade and Zwicky assumed that supernovae could be transforming a normal star into a neutron star after removing all the charged particles. However, the supernovae was not understood at the time.¹⁻³ This was the beginning of research in the physics of neutron stars.^{3,4} There were other works in the 1930s that went in the direction of exploring the possibility of regular stars with a deteriorating core. In particular, Oppenheimer and Volkoff (1939) proposed the state equation relative to the gas of neutrons. It became the basis on which later works were built.³

Indeed, neutron stars were discovered in the 1960s as pulsars by Jocelyn Bell and Antony Hewish.^{3,4} Initially, they interpreted them as references to extraterrestrial civilizations, but later they discovered that pulses are a feature of matter Stellar in severe extreme conditions.⁴ Neutron stars are the result of the evolution of massive stars ($M > 8M_S$), where the principal is unable to support its iron nuclei with hydrostatic pressure, often resulting in a supernova⁵ which is a bright and short-lived stellar explosion. Few of them have been observed historically,³ and

from the remnants of the blast produces neutron stars.^{3,5,6}

The importance of studying neutron stars lies in their unique properties, which are difficult to find or reproduce on Earth or in the solar system. Neutron stars are very dense stars^{2,6} making them a unique laboratory for cold and dense materials that cannot be produced in terrestrial laboratories. Based on an understanding of matter's properties within these stars, our knowledge of matter and its behaviors will increase, especially in extreme conditions, to prove theories in high energy physics, particle physics, nuclear structure and cosmology.

Like other ordinary stars, We expect that there will be a spectrum of densities, from the iron core's density on the star's surface to several times the density of natural nuclear materials ($2.7 \times 10^{14} g/cm^3$) in the core in neutron stars and very diverse magnetic fields² (their classes and its characteristics will explain in section 1.3).

1.2 Magnetic field of neutron stars

Before the discovery of an intermittent radio emission from the Sun in the last century, the largest amount of magnetic fields (B) in the universe was unknown. Magnetic field on the sun is estimated to be several thousand Gauss (G), later it was found that the fields are extensive.⁷ Now it is known that there are stars with a magnetic field of up to $10^{13}G$ like the star (HerX1 pulsar) and the most in the neutron-magnetic stars where the field reaches $10^{17}G$.^{7,8} Researchers claim that it is possible; theoretically, that the field strength may be increased to $10^{32}G$.⁷ In 1956, Prendergast predicted that a stable magnetic field through a star can consists of a polar dipole part which is made stable by a toroidal part of similar strength. This concept is used in designing fusion reactors. It became possible to follow the development of an arbitrary field with numerical magneto-hydrodynamics. The

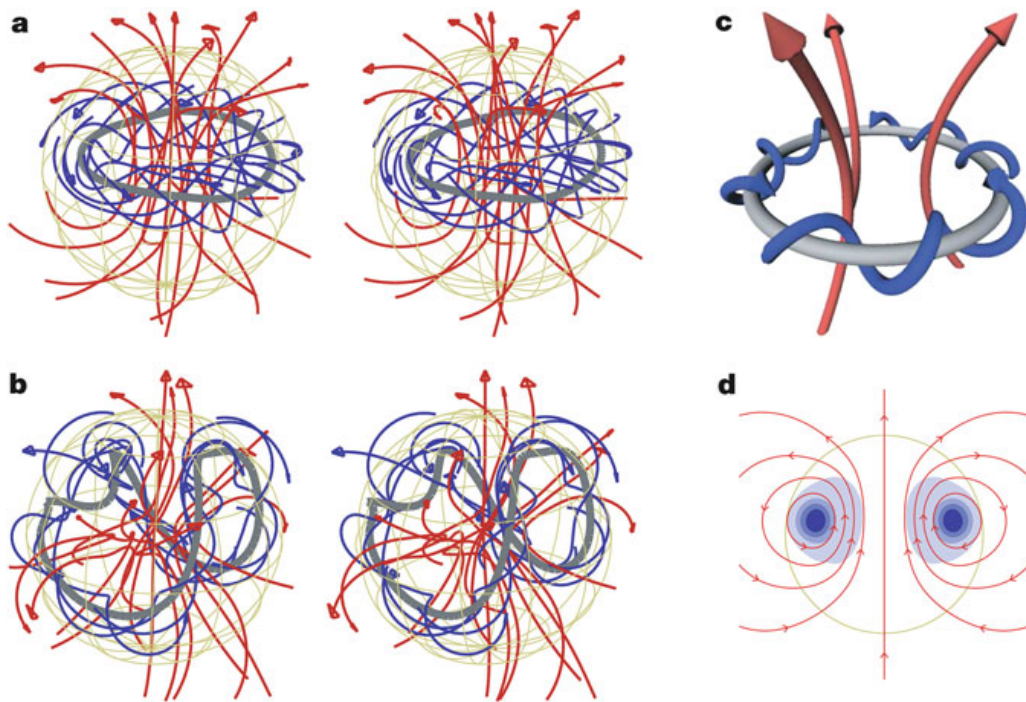


Figure 1.1: The magnetic field structure of a neutron star in a twisted ring formation.⁵

main result of this work is the emergence of a stable field formation in which the stable field is nearly axisymmetric and contains poloidal and cyclic components of similar strength. The shape of the resulting field is always the same; a ring torus shaped configuration fixed inside the star, with an almost dipole field attached to it outside the star. Majority of the field lines projected at the meridian plane are closed inside the star, but some extend outside it.⁹ As Figure 1.1, where image (a) is a stereoscopic view of twisted ring formation when the ring torus is trapped within a star, in the image (b), It reaches the surface of the star and it has many non axisymmetric patterns. Also, image (c) is an illustrative view of the magnetic field structure with different open field (red lines) and those in the ring torus confined inside the star (blue), and image (d) is the poloidal field lines (red) and the azimuthal mean of the toroidal field (blue).⁵

1.3 Types of neutron stars by the magnetic field

Nowadays, about 3,000 neutron stars are known since the first measurement of a neutron star. They have various characteristics, and composition¹⁰⁻¹² with ages ($\lesssim 100$ Myr),¹³ from magnetars to rotating radio transients. In addition to radio pulsars and central compact bodies,¹⁴ many other properties that can be used to classify them within classes and sub-classes,¹⁰ as detailed in Table(1.1).

Classes	sub-classes	Description
Rotation Powered Pulsars (RPP)	Classical Radio Pulsars (PSR)	
	Recycled Radio Pulsars	
	Rotating Radio Transients (RRAT)	
Accretion Powered Pulsars (APP)	High Magnetic Field Objects	(HMXB:XRP,SFXT)
	Low Magnetic Field Objects	(LMXB:AMXP,XRB)
Internal Energy-powered Neutron Stars (IENS)	Magnetars	(AXP/SGR)
	Compact Central Objects (CCO)	
	Isolated Neutron Stars (INS)	

Table 1.1: Classes and sub-classes of neutron stars by spin period P_s .¹⁰

Neutron stars can be classified into three main classes based on the magnetic field:

1. Rotating pulsars (RPPs): It was accidentally discovered by chance in 1968, known initially as radio pulsars, and operate with losing spin energy because of magnetic braking. The main characteristic of any pulsar are the following: spin period (P_s) and the period derivative (\dot{P}).¹⁰ Also, It is considered the largest class of isolated neutron stars (INS).¹⁵ The essential quantity derived is the surface magnetic field's dipole component; RPPs have three subcategories.

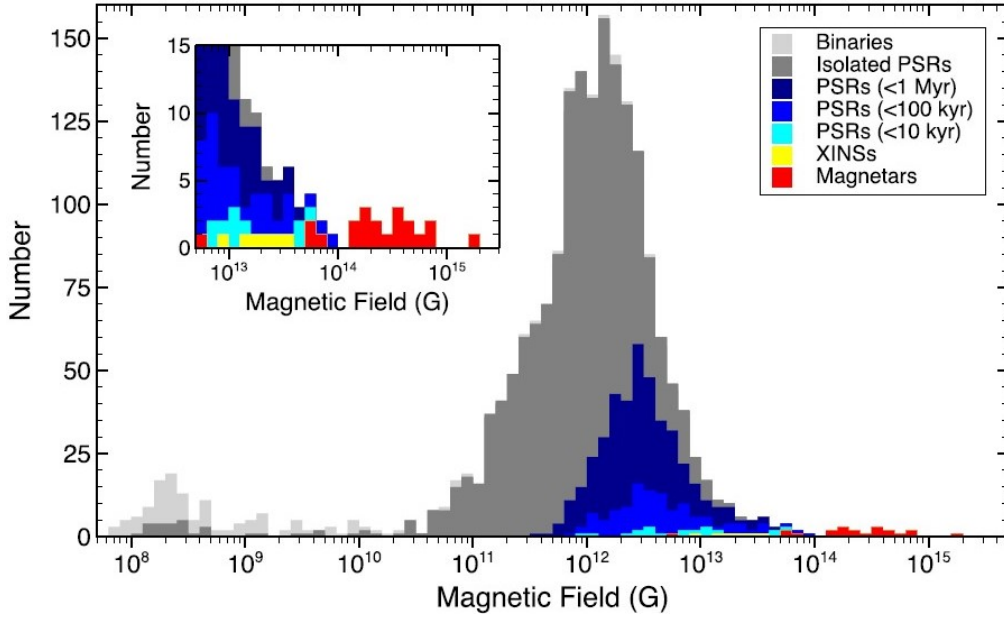


Figure 1.2: A graph showing the distribution in the magnetic field B of all radio, XINS, and magnetic pulsars for which \dot{P} was measured. Inner input: Zoom in to $B > 5 \times 10^{12}G$ to better show the distribution of magnets.⁸

The first sub-class is the classical radio pulsars (PSR) with $P_s \sim 1$ s and $B_s \sim (10^{11.5} - 10^{13.5})G$, and the second sub-class is the millisecond radio pulsars (MSRP), they are defined with $P \lesssim 20 - 30$ ms. The classification is not very precise because the condition is to separate a class of RPPs that have gone through various evolutionary paths that include long-life binary systems and a "recycle" accumulator loop that reduce the period of spin and the magnetic field. The third subclass Black Widow (BW) and Red Back (RB), stars form gateways to a specific class of binary MSRPs. It is so named because it is on its way to destroying its comrades by the strong winds of pulsars and will likely be left as isolated pulsars milliseconds.¹⁰

2. Accretion Powered Pulsars (APP): It is supported by the accumulation of material amounts from a companion and is classified as a low-mass X-ray binary (LMXB) or a high-mass X-ray binary (HMXB) depending on the donor star's mass, and it has two subcategories.

The first sub-class is neutron stars in HMXBs with $B_s \sim 10^{12}\text{G}$ usually appearing as X-ray stars. The accretion material's interaction with the neutron star's strong magnetic field is shown as complete popular absorption lines called cyclotron resonance scattering (CRSF) Which are distinguished in the stable X-ray of HMXBs. The magnetic field can be foredoomed from CRSFs, and neutron stars in LMXBs. The second subclass, have significantly weaker magnetic fields ($B \lesssim 10^{11}\text{G}$) by an extensive phase of accumulation.

Among all LMXBs comprising neutron stars - X-ray pulsars (AMXP) and accumulated milliseconds, X-ray anomalies (AMXB) are of interest as they are understood to be direct precursors of MSRPs and are expected to enter the radio pulsar phase when the accumulation ceases. The magnetic field in these systems is usually obtained based on an estimate of the internal truncation radius of the accretion disk as the disk pressure in this ray is balanced by the magnetic field pressure.¹⁰

3. Inner-powered neutron stars (IENS): It is an unclear power generation mechanism to this class. It is suspected to be related to internal processes, such as the decay of a strong magnetic field or the residual heat from the precursor.

Possibly the critical hyper-accretion phase occurs immediately after the birth of a neutron star, the original field was buried in deeper regions of the crust, the second subclass being the Seven Isolated Neutron Stars (INS), known as the Spectacular Seven stars, are optically faint and have X-ray spectra similar to the black body ($T \sim 10^6\text{K}$).¹⁰

The main focus of this thesis is magnetars. It includes a small group of X-ray pulsars considered to have the most magnetic fields. These neutron stars have surface fields $B \leq 10^{15}\text{G}$. Also, it was found that internal magnetic fields of approximately $B \sim 10^{17}\text{G}$.⁷ The strong X-ray emission of those objects ($L_x \sim$

10^{35} erg/s) appeared to be so loud and variable that they could not be given spin energy alone (as in radio pulsars), and there is no evidence of a companion in the star. Yet, in favor of any accumulation process⁶ (as binary x-ray systems).

Today about thirty magnetic and magnetic filter stars are known in the vicinity of the galaxy. Most of them appear as highly contrasting X-ray emitters, indicating an accumulation of a large amount of material while accumulating a high period. Anisotropy (varying in size according to the measurement direction) indicates that the accumulation either is not permanently stable and the magnetic field strength at these high values is subject to some temporal restructuring. Most of this magnetic activity is attributed to processes in the crust of a neutron star. At the same time, the core of the star is thought to be a Type II superconductor that may occasionally expel magnetic flux tubes, contributing to temporal oscillation.⁷

Due to these high B fields, the magnets' emission was thought to be triggered by their strong fields' atomization and instability. This robust X-ray output is usually modeled by thermal emission from the hot surface of a neutron star (about 3×10^6 K) reprocessed into a twisted magnetic envelope through resonant cyclotron scattering, a process only preferred under these extreme magnetic conditions.⁶

There are many interesting questions and problems regarding the crust and the basic structure in the presence of strong magnetic fields as has been deduced with respect to magnetic stars. Problems such as these have become the subject of recent investigations other than those discussed in this thesis.

It appears that the crust is not structured as a liquid. Relativistic hydrodynamics assumes that the strong magnetic fields in these neutron stars can cause matter in the crust not to the surface layer but also into the layers below the brittle outer crust. It becomes "noodle-like" vertically (to the surface) outside the stained structures, a substance that may mix with the super-fine liquid cells, and break down

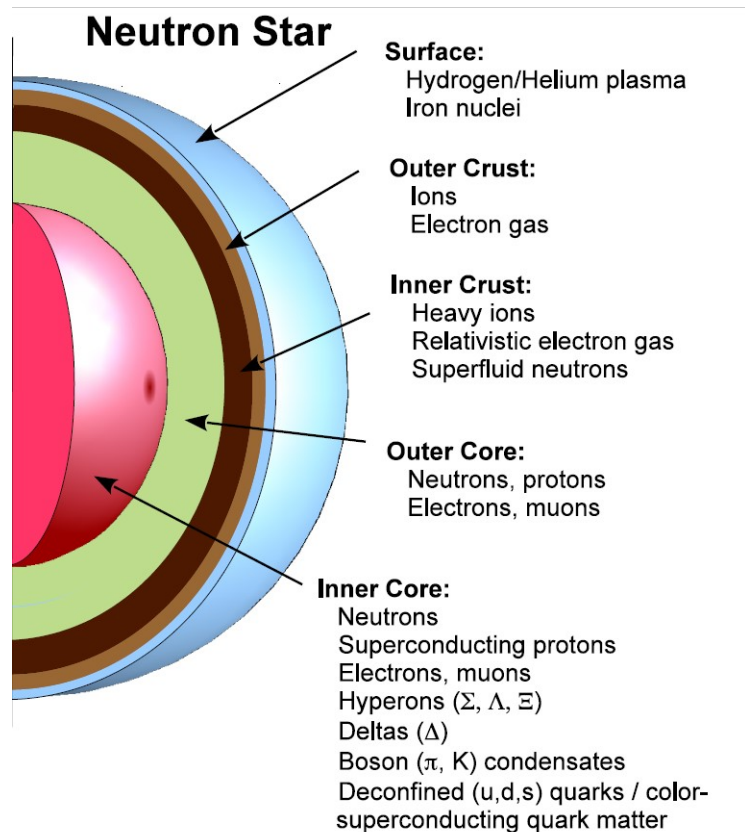


Figure 1.3: Internal structure of a neutron star.¹⁶

by magnetic flux tubes. These structures undergo plastic deformation that may generate magnetic activity in the magnets. The effect of such a structure on magnetic field distribution in the crust and neutron star environment remains unknown.⁷

Recent investigations of Strok 3D suggest that small magnetic fields of the Earth's crust may survive for an extended period of time in a similar fashion to the butterfly structure of sunspots. This happens in bands moving toward the equator where crustal currents can organize themselves into a strong equatorial electric line. Magnetic pressures of such fields and currents may lead to magnetic earthquakes and associated anomalies and temporal changes in the magnetic field up to a million years after the formation of the neutron star.⁷

1.4 Magnetic field and neutron star structure

There is a significant effort dedicated to investigate neutron star structure (Figure 1.3) and the effect of magnetic fields on it, especially the strong magnetic field, and during several years from the nineties to the current decade.^{17,18}

In 1995, Bokeh presented the first numerical solutions to Einstein - Maxwell equations describing fast spinning neutron stars with a magnetic field. These completely consistent and relativistic solutions and all the effects of the electromagnetic field on the equilibrium of the star (Lorentz force, spacetime curvature due to electromagnetic stress energy) are taken into account. Five formulas are used for the dense state, but the partial differential equation system was combined using the pseudo-spectra method. Various tests passed are presented by numerical code. Next, the effect of the magnetic field on the structure of neutron stars is studied, through the comparison of magnetic and non-magnetic formations with the same number of baryons. The star's deformation due to the magnetic field is significant only for huge values of B ($B > 10^{10}$ T). The maximum mass and the maximum rotational speed were calculated as the magnetic field increased.

The maximum permissible magnetic field for the poloidal is in the order of 10^{14} T and is reached when the magnetic pressure is similar to the pressure at the center of the star. For these values, it is found that the maximum mass of neutron stars increases by 13% to 29% (depending on EOS) to the maximum mass of non-magnetized stars.¹⁹

In 1999, Yuan and Zhang investigated the overall characteristics of dense neutron star matter and star structure under the effect of strong magnetic fields, based on two nonlinear models of nuclear material, i.e. BB and ZM, within an approximation of the mean-field. In contrast, to the results obtained in the linear

p-u model and the BB model, they found that the effect of the magnetic field on the effective nucleon mass m^* is not crucial in the ZM model. Therefore, they expected that neutrons within the neutron star has a probability of being a super-fluid in the ZM model if there was a strong value of the magnetic field within the star.

Moreover, the EOS equations will become smoother and softer as the magnetic field (B) increases. They show the effects of internal magnetic fields on the overall properties of neutron stars, such as critical masses, corresponding radius, moment of inertia, crust mass, and crust torque, Of inertia, and a red shift in gravity in both nonlinear p-u models.²⁰

In 2001 Cardal studied static neutron stars with polygonal magnetic fields and a simple class of electric current distributions compatible with stability requirements. Because this is a class of electric current distributions, they found that magnetic fields are too large to exist when stationary formations are present when the magnetic force releases enough mass off the center that the force of gravity points outward near the origin in the equatorial plane.

The state equations (EOS) applied in past work obtained higher block configurations than stated. It also delivers results with more modern EOS. All of the EOSs studied, they found that the largest mass between these static magnetic field configurations is significantly greater than the maximum mass that can be obtained through uniform rotation and that for constant values of the baryon number, all the maximum mass configurations are characterized by an off-center density maximum.²¹

In 2003, Mao studied the effects of strong magnetic fields on the structure of a neutron star. If the inner field is in the same order as the surface field currently observed, the magnetic field affecting the star's mass and radius is negligible. If one believes that the internal magnetic field can be as large as measured from numerical

viral theory, then significant effects can be induced. The stars' maximum mass arose mainly, while the central density was mostly retreated. For two stars of equal mass, the magnetic star's radius could be about 10%20% than the nonmagnetic star.²²

In 2011, Ryu and Cheoun investigated the effect of the intensity-dependent magnetic moment of baryons in the strong magnetic fields of a neutron star with hyperons and kaons. In the presence of strong magnetic fields, charged particles exhibit Landau quantization, so that the chemical potential, state equation, and mass-half relationships depend on the strength of the magnetic fields.

Since the magnetic fields are integrated with the magnetic moments of the baryons, they compute the neutron star with Hyperons and kaon condensation and investigate the effect of the intensity-dependent magnetic moment of eight baryons obtained by the quark - meson coupling model. The effect is a maximum of 0.1M for hypertonic matter, but in cosmic matter, its effect can be ignored.²³

In 2013, Bordbar and Rezaei studied the effect of strong magnetic fields on the broad properties of neutron and proton stars. In their calculations, the neutron star material has been approximated from a pure neutron material. Using the lowest order finite contrast method at zero and infinitesimal degrees, and operating the AV18 potential, they presented the effects of strong magnetic fields on the gravitational mass, radius, and gravitational redshift of neutron and proton stars. It is found that the neutron star state equation becomes stiffer with increasing magnetic field and temperature. This leads to greater values of the maximum mass and radius of neutron stars.²⁴

In Figure3.2 one can see the behavior of the pressure with energy density in panels a and a*, while in panels b the relation of the star mass as a function of the radius for different values of magnetic field is plotted. In panel c the effect of temperature is examined.

- (a) Pressure (P) vs. energy density (e) relation is plotted at different values of magnetic field, where B is 0 G (continuous curve), 5×10^{18} G (dashed curve) and 10^{19} G (dash-dotted curve) at a constant temperature value, $T = 0$ MeV.
- (a*) Same as at the top but for a different set of energy densities.
- (b) Mass-radius relation, for the cases $B = 0$ G (continuous curve), $B = 5 \times 10^{18}$ G (dashed curve) and $B = 10^{19}$ G (dash-dotted curve) at a constant value of the temperature, $T = 0$ MeV.
- (c) Mass-radius relation, for the cases $T = 0$ MeV (solid curve) and $T = 15$ MeV (dashed curve) at a fixed value of the magnetic field, $B = 5 \times 10^{18}$ G.²⁴

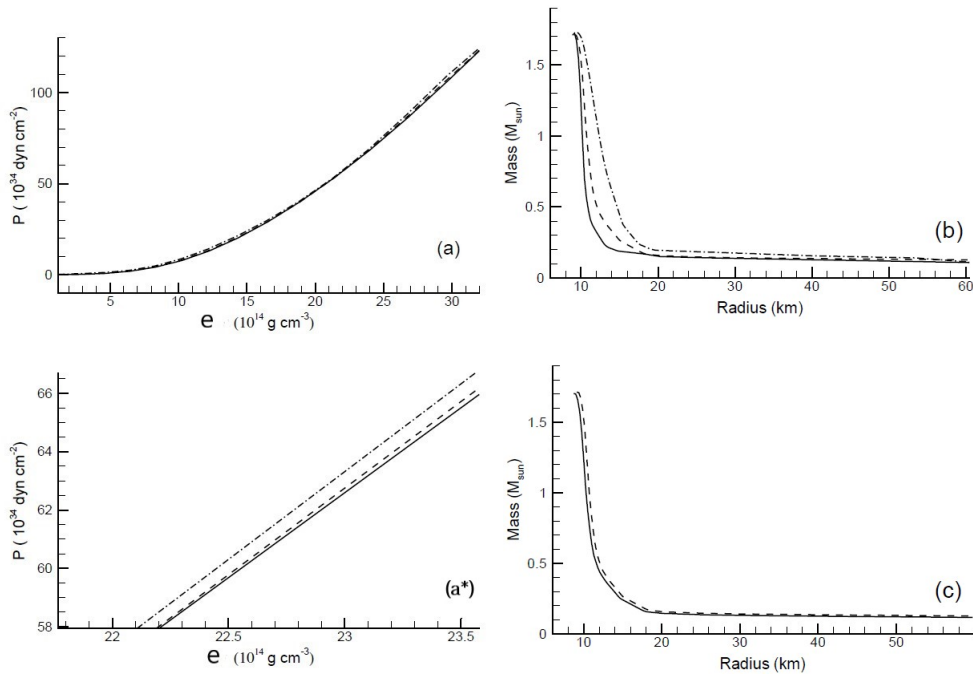


Figure 1.4: (a) Pressure (P) vs. energy density (e) relation is plotted at different values of magnetic field. (a*) Same as in the top but for a different range of energy density. (b) Mass-radius relation, relation is plotted at different magnetic field values. (c) Mass-radius relation, relation is plotted at different temperature values.²⁴

In 2016, Bucciantini and others discussed the properties of equilibrium models of magnetic neutron stars and showed how they can have both internal and external currents. These magnetic fields have also been discussed bearing in mind

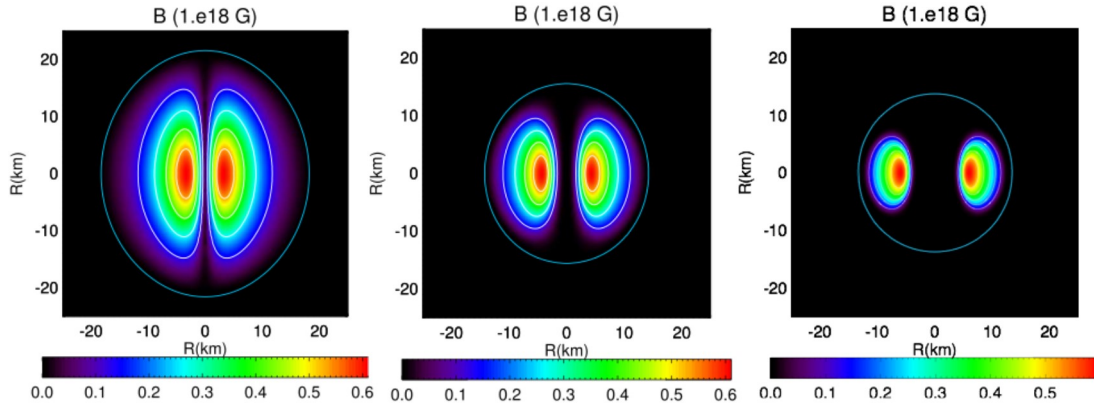


Figure 1.5: Neutron stars with a purely toroidal field. Portraits show the strength of the magnetic field for a star of mass $M = 1.68 M_{sun}$. From left to right $\gamma = 1, 2,$ and 4 . The blue line is the stellar surface.²⁵

their inherent stability. In the case of a twisted magnetosphere, they demonstrate how the torsion amount regulates the overall structure as shown Figure(1.5). The general solution rendering is dependent on the simultaneous numerical solution of Einstein's equations with equation of state $p \propto \rho^\gamma$ where ρ is rest mass density and γ is constant.²⁵

In the next chapter, we'll look at how to get the equations describing the star system, the forces that affect it, and the structure of the star. In Chapter 3, we systematically study magnetic field states on a neutron star. We show the effect of various magnetic fields on the star's dimensions, potential energy, and momentum.

Chapter 2: Formalism

2.1 System of Equations

First, we will present a self-consistent model for studying a neutron star structure in strong magnetic fields. We will start from a microscopic Lagrangian; this model includes the effect of the magnetic field on the equation of the state (EOS), then the interaction of the electromagnetic field with the material (magnetization). The loss of variation in the energy-momentum tensor, as well as the general relative aspects, depending on the work of D.Chatterjee et al. 2015,²⁶ Unless otherwise stated, we work with $c = \hbar = 1$ and a metric signature of $(-1, 1, 1, 1)$. The fundamental constants G and μ_0 will be kept in the equations for more good readability.

2.1.1 Energy-Momentum Tensor in the presence of a Magnetic Field

We will construct the microscopic energy-momentum tensor from the Lagrangian for fermions in an electromagnetic field; we will calculate the energy-momentum thermodynamic average tensor to identify the contributions by the magnetic field.

Without coupling with the electromagnetic field, in the general relative

context, it is generally assumed to have a perfect fluid form,

$$T^{\mu\nu} = (\varepsilon + p)u^\mu u^\nu + pg^{\mu\nu} \quad (2.1)$$

where ε denotes the (matter) energy density, p the pressure, and u^μ the fluid four-velocity.

The Lagrangian density of a fermion system can be written with a magnetic field such that

$$L = -\bar{\psi}(x)(D_\mu\gamma^\mu + m)\psi(x) - \frac{1}{4\mu_0}F_{\mu\nu}F^{\mu\nu} \quad (2.2)$$

where $D_\mu = \partial_\mu - iqA_\mu$, q is the charge of the particles, and the field strength tensor of the electromagnetic field,

$$F^{\mu\nu} = \partial^\mu A^\nu - \partial^\nu A^\mu \quad (2.3)$$

The condition determines the energy-momentum tensor of Einstein - Hilbert that appears as the source of Einstein's equations that the procedure, S , is constant,

$$S = \int L\sqrt{-g}d^4x \quad (2.4)$$

In our case, a fermion field associated with an electromagnetic field is given by

$$T^{\mu\nu} = -\frac{1}{\mu_0}F^{\mu\alpha}F_\alpha{}^\nu + \frac{1}{2}\bar{\psi}(\gamma^\mu D^\nu + \gamma^\nu D^\mu)\psi + g^{\mu\nu}L. \quad (2.5)$$

The thermal average for the energy-momentum tensor is given by

$$\langle T^{\mu\nu} \rangle = (\varepsilon + p)u^\mu u^\nu + pg^{\mu\nu} + \frac{1}{2}(F_\nu^\tau M^{\tau\mu} + F_\mu^\tau M^{\tau\nu}) - \frac{1}{\mu_0}(F^{\mu\alpha}F_\alpha{}^\nu + \frac{g^{\mu\nu}}{4}F_{\alpha\beta}F^{\alpha\beta}) \quad (2.6)$$

In the fluid rest frame (FRF), assuming a perfect conductor, the electric

field vanishes, and only the magnetic field b_μ is nonzero. The electromagnetic field tensor can then be expressed in terms of b_μ as

$$F_{\mu\nu} = \epsilon_{\alpha\beta\mu\nu} u^\beta b^\alpha \quad (2.7)$$

with the Levi-Civita tensor ϵ , associated here with the Minkowski metric, where the magnetization tensor is

$$M_{\mu\nu} = \epsilon_{\alpha\beta\mu\nu} u^\beta m^\alpha \quad (2.8)$$

with the magnetisation four-vector

$$m_\mu = \frac{x}{\mu} b_\mu \quad (2.9)$$

where x numerical quantity.

2.1.2 Electromagnetic equations

Following BGSM, we use MSQI coordinates (Maximal Slicing - Quasi- Isotropic coordinates) (t, r, θ, ϕ) , in which the metric tensor g takes the form¹⁹

$$g_{\alpha\beta} dx^\alpha dx^\beta = -N^2 dt^2 + A^4 \left[B^2 r^2 \sin^2 \theta (d\phi - N^\phi)^2 + \frac{1}{B^2} (dr^2 + r^2 d\theta^2) \right] \quad (2.10)$$

where N , N_ϕ , A , and B are four functions of (r, θ) , where $\nu := \ln N, \alpha := \ln A$, and $\beta := \ln B$.

The most general form of the electric 4-current j compatible with the premise of stationarity, axisymmetry, and circularity has The following components about (t, r, θ, ϕ) coordinates: $j = (j^t, 0, 0, j^\phi)$, and the corresponding electromagnetic field tensor F must be derived from a potential 1-form A with the following components $A_{\alpha} = (A_t, 0, 0, A_\phi)$:

$$F_{\alpha\beta} = A_{\beta,\alpha} - A_{\alpha,\beta} \quad (2.11)$$

The electric field \mathbf{E} and the magnetic field \mathbf{B} as measured by the observer O_0 are given by

$$\begin{aligned} E_\alpha &= F_{\alpha\beta}n^\beta \\ &= \left(0, \frac{1}{N} \left[\frac{\partial A_t}{\partial r} + N^\phi \frac{\partial A_\phi}{\partial r} \right], \frac{1}{N} \left[\frac{\partial A_t}{\partial \theta} + N^\phi \frac{\partial A_\phi}{\partial \theta} \right], 0 \right) \end{aligned} \quad (2.12)$$

$$\begin{aligned} B_\alpha &= -\frac{1}{2}\epsilon_{\alpha\beta\mu\nu}n^\beta F^{\alpha\beta} \\ &= \left(0, \frac{1}{A^2 B r^2 \sin\theta} \frac{\partial A_\phi}{\partial \theta}, \frac{1}{A^2 B \sin\theta} \frac{\partial A_\phi}{\partial r}, 0 \right) \end{aligned} \quad (2.13)$$

Note that a consequence of 2.13 is that the magnetic field lines lie on surfaces $A_\phi = \text{const}$. In non-relativistic studies, A_ϕ is usually called the magnetic stream function or magnetic flux function and is denoted a or A .

The source-free Maxwell equations $F_{[\alpha\beta;\gamma]} = 0$ are automatically satisfied by the form (2.11) of \mathbf{F} . The remaining Maxwell equations $F^{\alpha\beta}{}_{;\beta} = \mu_0 j^\alpha$ can be expressed in terms of A_t and A_ϕ as the Maxwell-Gauss equation

$$\begin{aligned} \Delta_3 A_t &= -\mu_0 \frac{A^4}{B^2} (g_{tt} j^t + g_{t\phi} j^\phi) - \frac{A^4 B^2}{N^2} N^\phi r^2 \sin^2 \theta \times \\ &\quad \times \partial A_t \partial N^\phi - \left(1 + \frac{A^4 B^2}{N^2} r^2 \sin^2 \theta (N^\phi)^2 \right) \times \\ &\quad \times \partial A_\phi \partial N^\phi - (\partial A_t + \partial N^\phi \partial A_\phi) \partial (2\alpha + \beta - \nu) \\ &\quad - 2 \frac{N^\phi}{r} \left(\frac{\partial A_\phi}{\partial r} + \frac{1}{r \tan\theta} \frac{\partial A_\phi}{\partial \theta} \right) \end{aligned} \quad (2.14)$$

and the Maxwell-Ampere equation

$$\begin{aligned}
\tilde{\Delta}_3 \tilde{A}^\phi &= -\mu_0 A^8 (j^\phi - N^\phi j^t) r \sin\theta \\
&+ \frac{A^4 B^2}{N^2} r \sin\theta \partial N^\phi (\partial A_t + N^\phi \partial A_\phi) \\
&+ \frac{1}{r \sin\theta} \partial A_\phi \partial (2\alpha + \beta - \nu),
\end{aligned} \tag{2.15}$$

where

$$\tilde{A}^\phi := \frac{A_\phi}{r \sin\theta}, \tag{2.16}$$

use has been made of the short notation $\partial\alpha\partial\beta := \frac{\partial\alpha}{\partial r} \frac{\partial\beta}{\partial r} + \frac{1}{r^2} \frac{\partial\alpha}{\partial\theta} \frac{\partial\beta}{\partial\theta}$

$$\Delta_2 := \frac{\partial^2}{\partial r^2} + \frac{2}{r} \frac{\partial}{\partial r} + \frac{1}{r^2} \frac{\partial^2}{\partial\theta^2} \tag{2.17}$$

$$\Delta_3 := \frac{\partial^2}{\partial r^2} + \frac{2}{r} \frac{\partial}{\partial r} + \frac{1}{r^2} \frac{\partial^2}{\partial\theta^2} + \frac{1}{r^2 \tan\theta} \frac{\partial}{\partial\theta} \tag{2.18}$$

$$\tilde{\Delta}_3 := \frac{\partial^2}{\partial r^2} + \frac{2}{r} \frac{\partial}{\partial r} + \frac{1}{r^2} \frac{\partial^2}{\partial\theta^2} + \frac{1}{r^2 \tan\theta} \frac{\partial}{\partial\theta} - \frac{1}{r^2 \sin^2\theta} \tag{2.19}$$

2.1.3 Energy-momentum tensor and Einstein equations

Under the present assumptions of a stationary, axisymmetric spacetime, the Einstein equations result in a set of four elliptic partial differential equations for the metric potentials defined in eq.(2.10):

$$\Delta_3 \nu = 4\pi G A^2 (E + S^i_i) + \frac{B^2 r^2 \sin^2\theta}{2N^2} (\partial N^\phi)^2 - \partial\nu\partial(\nu + \beta) \tag{2.20}$$

$$\tilde{\Delta}_3 (N^\phi r \sin\theta) = -16\pi G \frac{N A^2}{B} \frac{J_\phi}{r \sin\theta} - r \sin\theta \partial N^\phi \partial (3\beta - \nu) \tag{2.21}$$

$$\Delta_2 [(NB - 1)r \sin\theta] = 8\pi G N A^2 B r \sin\theta (S^r_r + S^\theta_\theta) \tag{2.22}$$

$$\Delta_2 (\nu + \alpha) = 8\pi A^2 S^\phi_\phi + \frac{3B^2 r^2 \sin^2\theta}{4N^2} (\partial N^\phi)^2 - (\partial\nu)^2 \tag{2.23}$$

E, J_i, S^i_j are quantities obtained from the so-called 3+1 decomposition of

the energy-momentum tensor.

In our case of eq.(2.6) describing a perfect fluid endowed with a magnetic field, including magnetisation effects, they can be written in axisymmetric stationary symmetries as:

$$E = \Gamma^2(\varepsilon + p) - p + \frac{1}{2\mu_0} [(1 + 2x)E^i E_i + B^i B_i], \quad (2.24)$$

$$J_\phi = \Gamma^2(\varepsilon + p)U + \frac{1}{\mu_0} \left[(A^2 B^r E^\theta - E^r B^\theta) + x B^i B_i U \right], \quad (2.25)$$

$$S^r_r = p + \frac{1}{2\mu_0} \left(E^\theta E_\theta - E^r E_r + B^\theta B_\theta - B^r B_r + \frac{2x}{\Gamma^2} B^\theta B_\theta \right), \quad (2.26)$$

$$S^\theta_\theta = p + \frac{1}{2\mu_0} \left(E^r E_r - E^\theta E_\theta + B^r B_r - B^\theta B_\theta + \frac{2x}{\Gamma^2} B^r B_r \right), \quad (2.27)$$

$$S^\phi_\phi = p + \Gamma^2(\varepsilon + p)U^2 \frac{1}{2\mu_0} \left[E^i E_i + B^i B_i + \frac{2x}{\Gamma^2} (1 + \Gamma^2 U^2) B^i B_i \right] \quad (2.28)$$

all other components of J_i and S^i_i being zero. x is the magnetisation, defined by eq.(2.9) and U is the physical fluid velocity in the ϕ direction, as measured by the Eulerian observer; it is given by

$$U = \frac{Br \sin\theta}{N} (\Omega - N^\phi) \quad (2.29)$$

2.1.4 Magnetostatic equilibrium

The equations for magnetostatic equilibrium can be derived from the conservation of energy and momentum, expressed as vanishing divergence of the energy-momentum tensor:

$$\nabla_\mu T^{\mu\nu} = 0 \quad (2.30)$$

This can be detailed as:

$$\nabla_\mu T^{\alpha\beta} = \nabla_\alpha T_f^{\alpha\beta} - F^{\beta\nu} j_\nu^{free} - \frac{x}{2\mu_0} F_{\sigma\tau} \nabla^\beta F^{\sigma\tau} \quad (2.31)$$

where $T_f^{\alpha\beta}$ represents the perfect-fluid contribution to the energy-momentum tensor; one can recognise the usual Lorentz force term, too, arising from free currents.

As in Bocquet et al. (1995), in the case of rigid rotation (Ω constant across the star), a first integral of the following expression is sought

$$(\varepsilon + p) \left(\frac{1}{\varepsilon + p} \frac{\partial p}{\partial x^i} + \frac{\partial v}{\partial x^i} - \frac{\partial \ln \Gamma}{\partial x^i} - F_{i\rho} j^\rho_{free} \right) - \frac{x}{2\mu_0} F_{\mu\nu} \nabla_i F^{\mu\nu} = 0 \quad (2.32)$$

let us first note that for the neutron star case with a magnetic field in beta-equilibrium and at zero temperature, the enthalpy is a function of both baryon density and magnetic field

$$h = h(n_b, b) = \frac{\varepsilon + p}{n_b} = \mu_b \quad (2.33)$$

Hence we have

$$\frac{\partial \ln h}{\partial x^i} = \frac{1}{h} \left(\frac{\partial h}{\partial n_b} \frac{\partial n_b}{\partial x^i} + \frac{\partial h}{\partial b} \frac{\partial b}{\partial x^i} \right) \quad (2.34)$$

In addition, the following thermodynamic relations are valid under the present assumptions

$$\frac{\partial h}{\partial n_b} = \frac{1}{n_b} \frac{\partial p}{\partial n_b} \quad (2.35)$$

$$\frac{\partial p}{\partial b} = m (= \sqrt{m^\mu m_\mu}) = -\frac{\partial \varepsilon}{\partial b} \quad (2.36)$$

And we obtain for the derivative of the logarithm of the enthalpy

$$\begin{aligned} \frac{\partial \ln h}{\partial x^i} &= \frac{1}{\varepsilon + p} \left[\frac{\partial p}{\partial n_b} \frac{\partial n_b}{\partial x^i} + \left(\frac{\partial p}{\partial b} - m \right) \frac{\partial b}{\partial x^i} \right] \\ &= \frac{1}{\varepsilon + p} \left(\frac{\partial p}{\partial x^i} - m \frac{\partial b}{\partial x^i} \right) \end{aligned} \quad (2.37)$$

we assume that matter is a perfect conductor ($A_t = \Omega A_\phi$ inside the star); and it is possible to relate the components of the electric current to the electromagnetic

potential A_ϕ , through an arbitrary function f , called the *current function*:

$$j^\phi - \Omega j^i = (\varepsilon + p)f(A_\phi) \quad (2.38)$$

Under these two assumptions, the Lorentz force term becomes

$$F_{i\rho} j^\rho_{free} = (j^\phi - \Omega j^i) \frac{\partial A_\phi}{\partial x^i} = -(\varepsilon + p) \frac{\partial M}{\partial x^i} \quad (2.39)$$

with

$$M(r, \theta) = - \int_0^{A_\phi(r, \theta)} f(x) dx \quad (2.40)$$

then

$$\ln h(r, \theta) + \nu(r, \theta) - \ln \Gamma(r, \theta) + M(r, \theta) = \text{const.} \quad (2.41)$$

2.1.5 TOV and TOV-like Systems

Bowers and Liang have derived the resulting coupled system of equations for the star's structure²⁷ and reads

$$\frac{dm}{d\bar{r}} = 4\pi\bar{r}^2\varepsilon, \quad (2.42)$$

$$\frac{d\Phi}{d\bar{r}} = \left(1 - \frac{2Gm}{\bar{r}c^2}\right)^{-1} \left(\frac{Gm}{\bar{r}^2} + 4\pi G \frac{p_r}{c^2} \bar{r}\right), \quad (2.43)$$

$$\frac{dp_r}{d\bar{r}} = \left(\varepsilon + \frac{p_r}{c^2}\right) \frac{d\Phi}{d\bar{r}} + \frac{2}{\bar{r}}(p_\perp - p_r), \quad (2.44)$$

where $m(\bar{r})$ is the total mass enclosed in the sphere of radius \bar{r} , $\Phi(\bar{r})/c^2$ is the Newtonian gravitational potential, ε is energy density, p_r and p_\perp are the radial and tangential pressure components.

As discussed in the introduction, it is fundamentally inconsistent with solving spherically symmetric equations for magnetized neutron-star models since it

completely neglects the star's deformation due to the electromagnetic field. However, it is tempting to have a simple approach at hand, which allows us at least to reproduce the effects of the magnetic field on qualitatively (some) neutron-star properties by performing calculations only slightly more complicated than solving TOV equations. To that end, we modify the TOV system by adding the contribution from the magnetic field to the energy density and a Lorentz force term to the equilibrium equation:

$$\frac{dm}{d\bar{r}} = 4\pi\bar{r}^2 \left(\varepsilon + \frac{b^2}{\mu_0} \right), \quad (2.45)$$

$$\frac{d\Phi}{d\bar{r}} = \left(1 - \frac{2Gm}{\bar{r}c^2} \right)^{-1} \left(\frac{Gm}{\bar{r}^2} + 4\pi G \frac{p}{c^2} \bar{r} \right), \quad (2.46)$$

$$\frac{dp}{d\bar{r}} = \left(\varepsilon + \frac{b^2}{\mu_0} + \frac{p}{c^2} \right) \left(\frac{d\Phi}{d\bar{r}} - L(\bar{r}) \right). \quad (2.47)$$

b is the norm of the magnetic field, and $L(\bar{r})$ denotes here the Lorentz force contribution.^{28,29}

2.2 Numerical Solution

2.2.1 Poisson-like Partial Differential Equations Solution

We used LORENE code, which using spectral methods for solving Poisson-like partial differential equations which develop in Einstein-Maxwell system eqs(2.28), (2.14) and (2.15). Including modified inclusion of new magnetization terms, where, depending on the magnetization x defined in eq. (2.15), in these partial differential equations as shown in eq. (2.41), the expression for fluid's equilibrium does not change in the fields of gravity and magnetism.

The difference with Bocquet¹⁹ comes from using EoS which gives all required variables ε, p, x, n_b ; depending on two parameters: enthalpy h and magnetic field amplitude $b = \sqrt{b_\alpha b^\alpha}$ in FRF.

The free physical parameters that enter our model are: EoS, current function f (2.15), spin frequency and logarithm of central enthalpy $H_c = \log(h(r = 0))$. Once the equilibrium configuration has been calculated, global quantities are obtained either from the approximate behavior of the gravitational field (e.g., the gravitational mass M_G) or from the integral over the size of the star (the baryonic mass M_B) and the electromagnetic field (the magnetic moment \mathcal{M}).

2.2.2 TOV-like System Solution

In contrast to the previous subsection method, we solved a TOV-like system using the Fourth-Order Runge-Kutta Methods; Runge-Kutta methods are one-step methods. But, with multiple stages in each step. They are stimulated by relying on the Taylor methods. These new methods do not need derivatives of the right-hand side function $f(t, y(t))$ in the code and are thus general-purpose primary value problem solvers. The Runge-Kutta methods are among the most popular ODE solvers. Carl Runge and Martin Kutta first taught it around 1900. Modern developments are mostly by John Butcher in the 1960s.

The general first-order ODE system are³⁰

$$p'(x) = f(x, p(x)) \quad (2.48)$$

The classical Fourth-Order Runge-Kutta Methods is given by

$$p_{n+1} = p_n + h \left[\frac{k_1}{6} + \frac{k_2}{3} + \frac{k_3}{3} + \frac{k_4}{6} \right], \quad (2.49)$$

with $k_1 = f(x_n, p_n)$,

$$k_2 = f\left(x_n + \frac{h}{2}, p_n + \frac{h}{2}k_1\right),$$

$$k_3 = f\left(x_n + \frac{h}{2}, p_n + \frac{h}{2}k_2\right),$$

$$k_4 = f(x_n + h, p_n + hk_3).$$

The k_1, k_2, k_3 , and k_4 are known as stages of the Runge-Kutta method. They correspond to different estimates for the slope of the solution. Note that $p_n + hk_1$ corresponds to an Euler step with stepsize h starting from (x_n, p_n) . Therefore, k_1 corresponds to the slope of the solution one would get by taking one Euler step with stepsize h starting from (x_n, p_n) .³⁰

Chapter 3: Neutron Stars: Properties results

3.1 Magnetic Field Profile

Based on the numerical solution of the equations obtained in Chapter 2 using LORENE Code, we built a (table EoS) to create the magnetic field profile and other properties after entering the equation of the state table's initial properties.

Based on the results obtained with the computer code: The shape of the magnetic field lines and the radius of the star change with the change of the central enthalpy (H_c). In Figure (3.1), we plot the magnetic field lines for different values of Central Enthalpy. WE start with a small value and increase it through the different panels of the figure. We can see that when the amount of the central enthalpy is small, the field lines that are close to the center are parallel and straight, and with the increase in the value of the central enthalpy, the curvature, and expansion of the field lines increases outward. As for the radius, the change is noticeable when the central enthalpy changes from a very small value $H_c = 0.01c^2$ to $H_c = 0.1c^2$, where the enthalpy doubled ten times, and the radius doubled approximately one time. If the enthalpy changes, It did not change the shape of the magnetic field lines in the star only and their magnitude it also changes the maximum value was in

panel a by $3.057 \times 10^{16}G$, while in Figure (3.1 b) is increased by $2.324 \times 10^{17}G$. The amount of the maximum value in Figure (3.1 c) triple the enthalpy, where it became $H_c = 0.3c^2$, and the magnitude of the magnetic field became $5.036 \times 10^{17}G$ and also became $7.035 \times 10^{17}G$ When the central enthalpy reaches $H_c = 0.5c^2$ in Figure(3.1d).

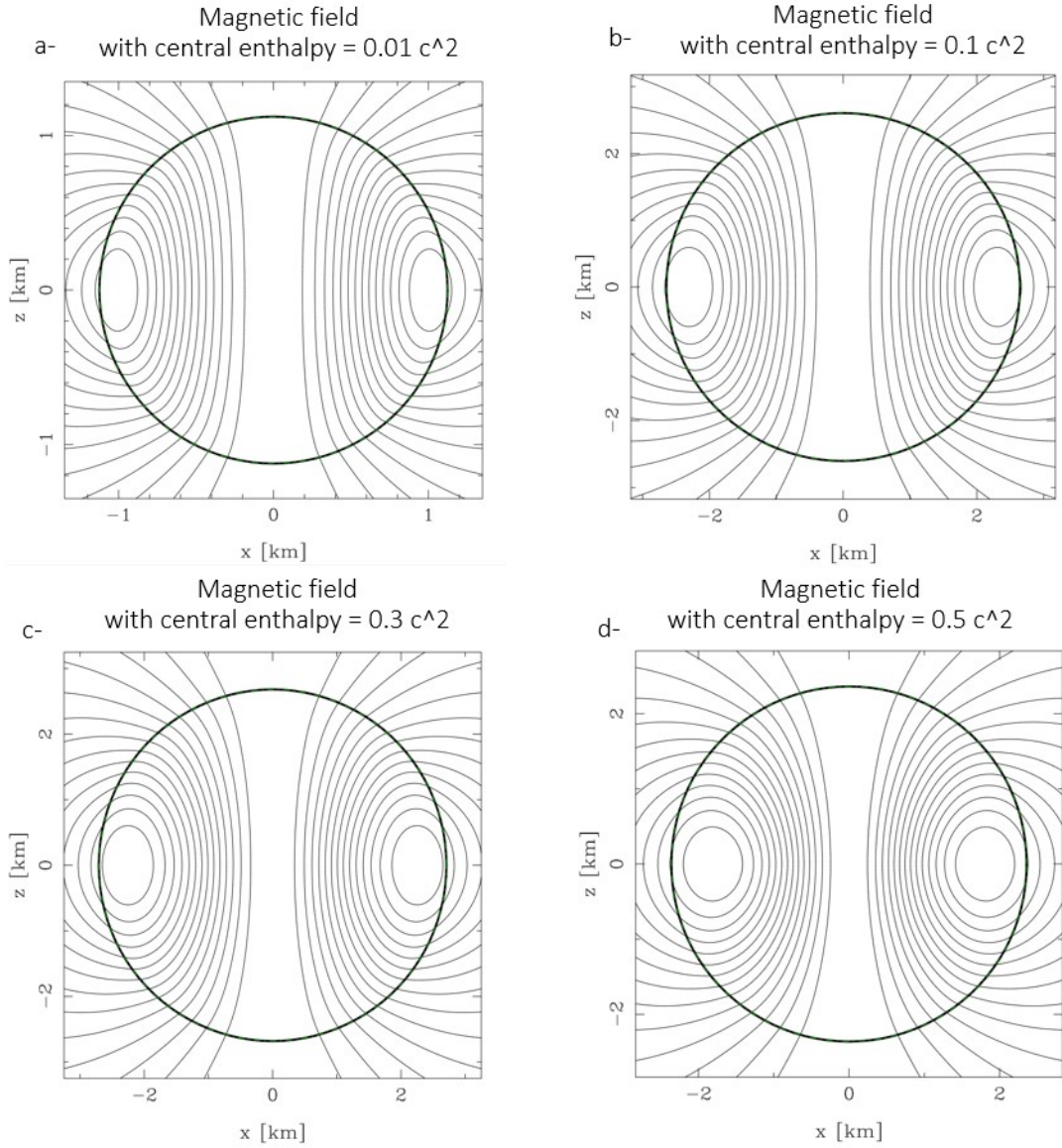


Figure 3.1: Magnetic field lines in the plane (x, z) of $M_G = 3M_\odot$ Neutron star model is equipped with a magnetic field B and a unique EoS table (see EoS of Table) with the difference in the value of the central enthalpy [c^2] 0.01, 0.1, 0.3, 0.5 in a, b, c, d in series. The bold line indicates the surface of the star and the magnetic moment is along the z-axis.

Based on these results, it is apparent that the enthalpy in the neutron star controls the distribution and shape of the magnetic field lines, where the highest value the central enthalpy, the more significant the curvature and expansion of the lines. In addition to a positive increase in the magnitude of the magnetic field, and its maximum value with the increase of the central enthalpy, one also can see that the radius of the star increases in the same manner but at a lower rate.

As the magnetic field changes with the central enthalpy, the magnetic field norm rings' shape changes with the central enthalpy (H_c). The magnetic field norm consists of three main rings: a central rings and two other rings beside the center. In Figure (3.2 a), the central enthalpy is very small, but the central rings of the field norm is large, and the other rings are very small. With the increase in the central enthalpy's value, the curvature and expansion of the norm rings beside the center increases. While in Figure (3.2d), the side rings become more apparent for the one before them, and the central ring is close in shape to the side rings, which differs in Figure (3.2b and 3.2c). One can notice that the central ring starts to be more like a circle, and the with the increment of H_c it starts to deform in shape and deviate from circular shape. Consequently, the neutron star's enthalpy controls the distribution and shape of the magnetic field norm rings, where the largest value of the central enthalpy, the central rings contract and the side rings expand.

Since the magnetic field and the magnetic field norm are affected by central enthalpy, enthalpy is in the star as a whole, according to Figure (3.3). The greater the central enthalpy, the more intense the isocontour rings that express the enthalpy distribution in the neutron star entered the star, while outside the star, the density of the dashed lines decreased.

Generally, We also note that the rings' shape changes inside the star with the central enthalpy change. In Figure (3.3a), the rings were circular and regular. The

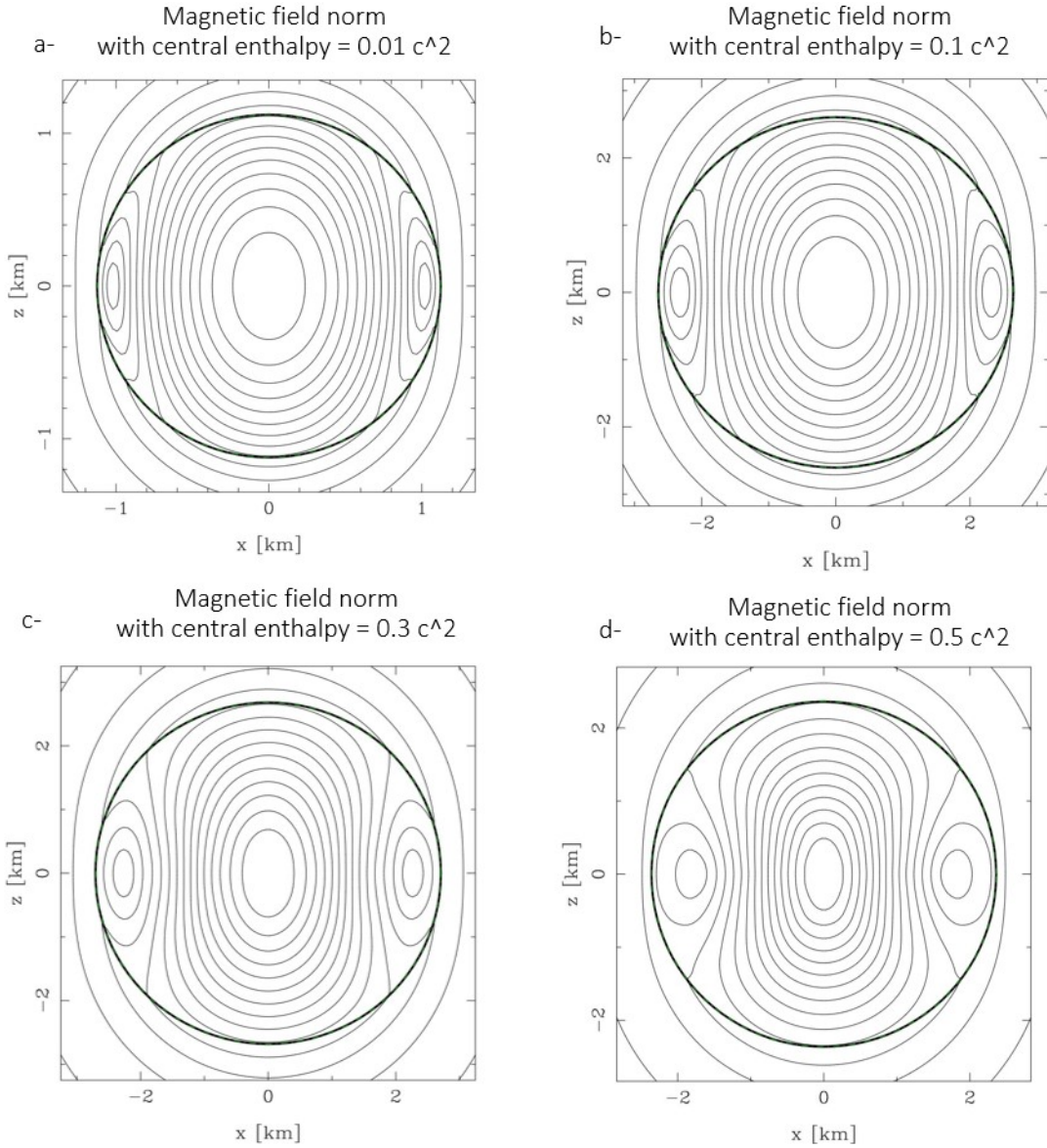


Figure 3.2: Magnetic field norm rings in the plane (x, z) of $M_G = 3M_\odot$ Neutron star model is equipped with a magnetic field B and a unique EoS table (see EoS of Table) with the difference in the value of the central enthalpy [c^2] 0.01, 0.1, 0.3, 0.5 in a, b, c, d in series. The bold line indicates the surface of the star and the magnetic moment is along the z -axis.

farther from the center, the rings converged more due to the decrease in the central enthalpy amount and the lack of field lines in the center, and the maximum value of the magnetic field Very little. but in Figure (3.3 b), the isocontour rings become horizontal elliptical and become more convergent, and the density of the rings is higher due to the large increase in the enthalpy from $H_c = 0.01$ to $H_c = 0.1$. However,

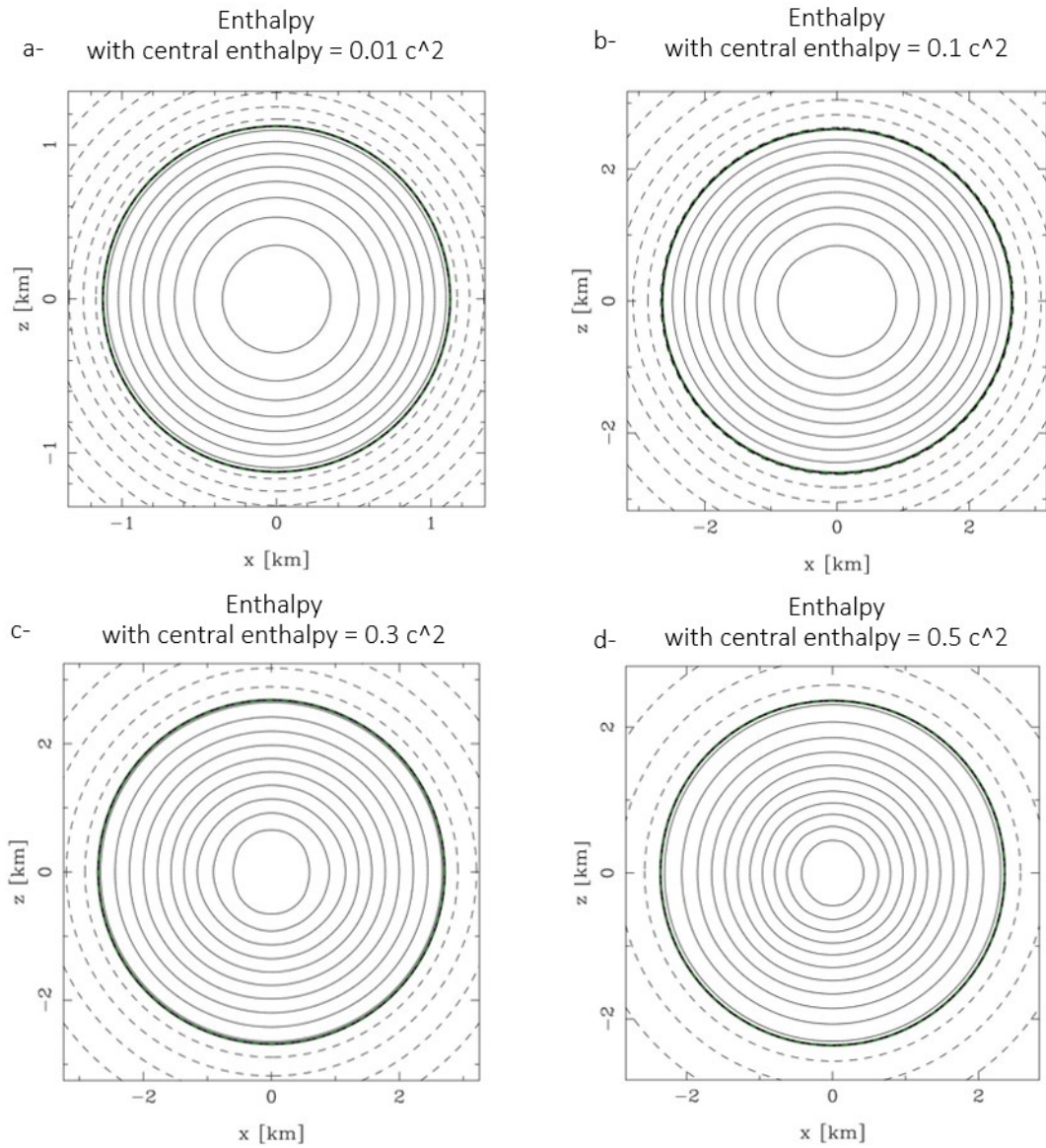


Figure 3.3: Enthalpy isocontours in the plane $((x, z))$ of $M_G = 3M_\odot$, the solid rings represent positive enthalpy isocontours, dashed rings negative ones (no matter).

with the increase of the central enthalpy, the contour rings' density increases, and their diameter decreases, but it becomes horizontal elliptical due to the curvature of the field lines and the change in the energy distribution. However, this does not change the physical meaning because it depends on identifying the axes only, as in Figure (3.3c). In the end, with the height of the central enthalpy and the magnitude of the magnetic field greatly, the isocontour rings become very close, smaller, and

regular circular as in Figure (3.3d).

We conclude from the above that biconvex contour rings change in terms of their density, size, and shape, the density of the contour rings increases directly with the increase of the central enthalpy and the magnetic field, their size decreases, and their shape changes according to the curvature of the magnetic field lines, especially at high magnetic fields, as in Figure (3.3 d).

Thus, we have tested the construction of the magnetic field profile, and we will depend on the results of the larger magnetic field as it depends on Figure(3.1d,3.2d, and 3.3d) that we will use it in solving TOV-like equations and identifying the properties of mass and pressure.

3.2 Structure of Neutron Star

In this section, we will discuss the change in the mass and pressure properties of a neutron star that has a high magnetic field and adopt several shapes of the magnetic field norm $b_l(x)$ for comparison and understanding how these properties change with $x = r/r_{mean}$, the ratio between the radius \bar{r} in Schwarzschild coordinates and the star's mean (or areal).

We will examine four forms of the magnetic field norm, which are the absence of a field, a static field, an increasing variable field, and a contradictory variable field, which are illustrated in the following $b = 0, b = constant$,equations(3.1, 3.2) where $b_c = 5 \times 10^{15}G$, as shown Figure (3.4) based on Chatterjee, 2019.²⁸

$$b_0(x) = b_c \times (1 - 1.6x^2 - x^4 + 4.2x^6 - 2.4x^8), \quad (3.1)$$

$$b_2(x) = b_c \times (1.1x - 0.1x^2 + 2.2x^3 - 0.7x^4 - 1.3x^5 - x^6). \quad (3.2)$$

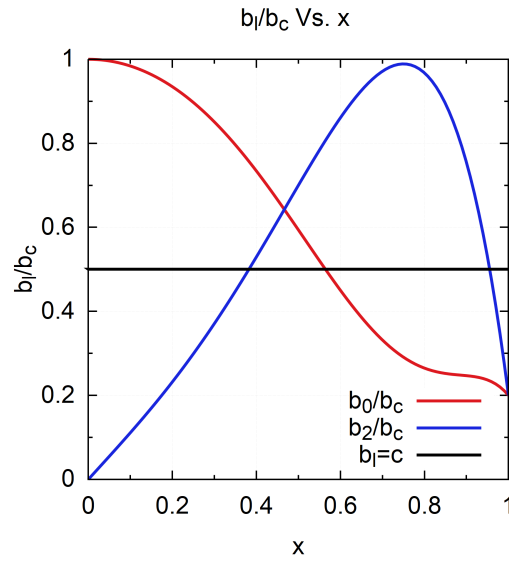


Figure 3.4: Several shapes of the magnetic field norm $b_l(x)$

To understand the behavior and effect of a magnetic field norm on mass and pressure; We divided the mass and pressure by the maximum values in each case, compared them, and took the magnetic field norm on which our magnetic field profile depends.

After solving the equations, we noticed a distinct differences of mass change with the star's radius, as in Figure (3.5 left), especially the rate of change (the slope of the tangent to the curve), which we will rely on in the comparison. In the absence of a magnetic field, which is a hypothetical case, the change in the tangent to the curve (black) at the beginning is more noticeable. When x approaches one (close to a star's surface), the tangent slope is almost fixed. i.e., the change in the matter is proven.

In this case, it is due to the effect of chaos. The effect of attraction is more regular after the concentration of most of its mass and depends on the radius (the distance between two masses, as in Newton's law of general attraction) linearly as observed. However, in the case of a constant magnetic field, we notice that the tangent change to the curve (red) has become slower than The absence of the field.

This means that the change of matter inside the star becomes less than, and the matter is distributed more.

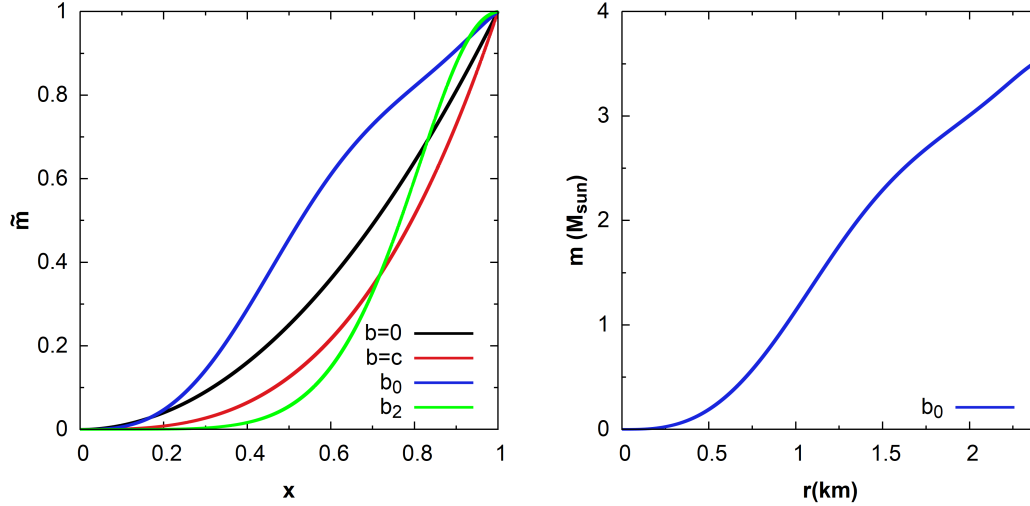


Figure 3.5: (left) $\tilde{m} = m/m_{max}$ vs. $x = \bar{r}/r_{mean}$. (right) mass $m(M_{sun})$ vs. radius $r(km)$.

The most important thing we want to know is the characteristics of the material distribution with the most realistic magnetic field that b_0 is expressed in the blue curve; We notice an exact change in the behavior of the curve from the previous cases, where the slope change is initially slow, then the rate of change of the slope increases and is constant between 0.3 and 0.5. It changes between 0.5 and 0.8 non-linearly and then becomes slower and more stable. In comparison with a changing magnetic field (green), we notice that the change in inclination is very different and does not give expected results, where the rate of change of the tilt, i.e., the change of the matter concerning the radius, is minimal until it approaches the middle of the star. However, it is expected that most of the matter, which will be concentrated in the star's core, as we indicated in the foreground.

We conclude from the preceding that the behavior of the $\tilde{m}-x$ curve, which expresses the change of mass within the neutron star, changes with the presence or absence of several forms of the magnetic field, where it is more variable and more

realistic with b_0 , in which the distribution of matter is denser than. In the star's core, but with the increase in the force of gravity and the magnetic force, the change in the mass (matter) becomes more stable. Furthermore, with the increase is in the intensity of the magnetic field compared with the gravity (the amount of matter), the distribution changes, but it is fixed when approaching the surface of the star as expressed in Figure (3.5 Right).

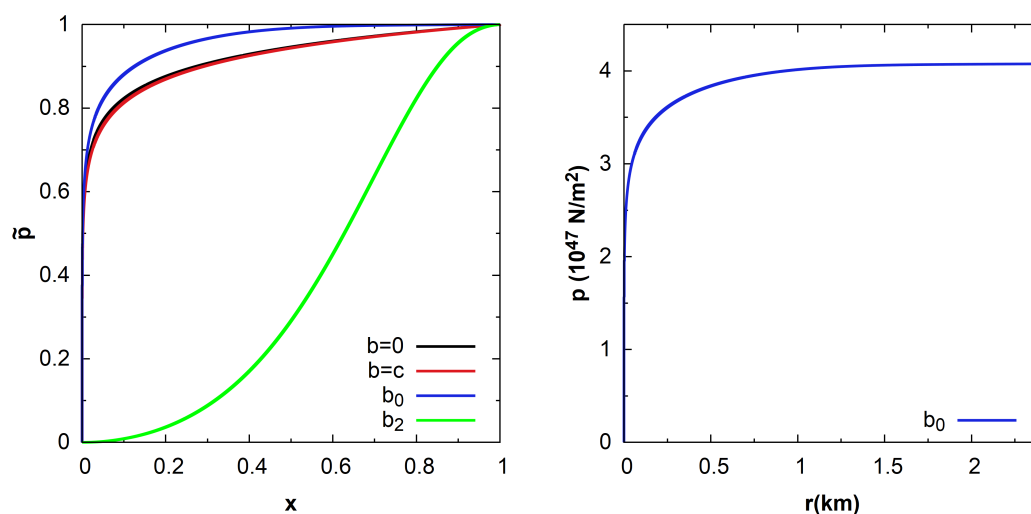


Figure 3.6: (left) $\tilde{p} = p/p_{max}$ vs. $x = \bar{r}/r_{mean}$. (right) pressure $p(10^{47} \text{ N/m}^2)$ vs. radius $r(\text{km})$.

Another property that we study is pressure. We notice that the changes in pressure with different magnetic fields are less, as shown in Figure (3.6 left), except for the hypothetical variable magnetic field (green). In the loss of a magnetic field, we notice that the change in the inclination of the curve at the beginning is tremendously rapid, and this is normal due to the presence of matter in the core of the star, and then the pressure gradually decreases to become more stable for the radius (black), i.e., when approaching the surface. With a fixed magnetic field, there is a displacement in the curve. The change in the slope decreases faster. It proves the curve's slope in the same way (red) due to the influence of the static magnetic field.

As a mass, the most important thing we want to know is that pressure is affected by a magnetic field, exceptionally the most realistic, which is expressed by b_0 in the blue curve; We notice an exact change in the behavior of the curve from the previous cases, where the change in the slope is at first very fast and continues more with the increase of x (inside the star). The slope rate slowly decreases between 0.1 and 0.2, and then it changes between 0.2 and 0.4, respectively. Non-linear and then slower and slope close to zero. In comparison with a changing magnetic field (green), we notice that the change in inclination is very different and does not give expected results, where the rate of change of inclination, i.e., the change in pressure for the radius, is meager until it approaches the middle of the star. However, it expected that most of the matter, which will be concentrated in the star's core, as we indicated in the foreground.

We conclude from the previous that the behavior of $\tilde{p} - x$ curve, which expresses the change in pressure inside the neutron star, changes with the presence or absence of several forms of the magnetic field. Where it is more variable and more realistic with b_0 , in which the pressure is more in the core of the star, but with the increase in the force of gravity and the magnetic force becomes more, the change in pressure becomes almost non-existent (i.e., the pressure is constant) when approaching the surface of the star as it crosses the Figure (3.6 right).

Chapter 4: Conclusions

The study of neutron stars is significant to understand the properties of matter in conditions different from Earth, where the density of matter and energy is high, and the magnetic field is strong. In this study, We investigated to study the contribution and effect of the magnetic field on the neutron star structure. This model considers a system consisting of attractive protons confined to finite relative space and with a magnetic field. We constructed the state equation so that the material is denser and depends on the magnetizing properties. Also, we used the solution of the Poisson-like partial differential equations that were developed in the Einstein-Maxwell system to determine the shape of the magnetic field lines, the standard magnetic field, and the bifurcation, and select the largest magnetic field possible depending on the central enthalpy. We also used differential TOV-like rates to find the relationship of mass and pressure with the star's dimensions.

Our neutron star structure is described by many parameters such as bifurcation, material density, and magnetic medium. The other parameters describe the magnetic field structure and other physical properties.

These elements play a significant role in the magnetic field's bends within the neutron star and the system's energy. We note that the variable standard magnetic field characteristically affects the material's properties for the systems considered here.

Our results indicate that the magnetic field plays an essential role in forming the neutron star, whether in its radius or distributing the material (mass) and the pressure inside it. The central elongation controls the magnetic field, composition of the magnetic field profile, and system state. Most importantly, the magnetic field properties significantly impact the mass and pressure, as the distribution of the material inside the star changes and are centered in the core. Its distribution in several stages (layers) sometimes according to the magnetic field's shape and in each case, especially in the most realistic cases. Our simulations suggest that the mass distribution is always variable and dimensional in the static magnetic field. On the contrary, the change in the mass distribution in the case of the changing magnetic field (more realistic) in stages and within periods as we explained in Chapter Three and this applies to the change of pressure, but the effect of the change of the magnetic field on it is less noticeable.

In future work, more complications could be added to our model. This includes considering the presence of diversity in the matter and the internal interaction between them. Moreover, we can investigate the effect of a strong magnetic field on a neutron star structure and solve the system equations in full without neglecting variables such as the change in the gravitational coefficient and other internal forces.

References

- (1) Viganò, D. Magnetic fields in neutron stars, 2013.
- (2) Bandyopadhyay, D. *Journal of Astrophysics and Astronomy* **2017**, 38.
- (3) Robertshaw, O. In, 2010.
- (4) Takibayev, N.; Boshkayev, K., *Neutron stars: physics, properties and dynamics*, OCLC: 962852870, 2017.
- (5) *The Physics and Astrophysics of Neutron Stars*; Rezzolla, L., Pizzochero, P., Jones, D. I., Rea, N., Vidaña, I., Eds.; Springer International Publishing: 2018.
- (6) Rea, N. *Proceedings of the International Astronomical Union* **2012**, 8, 11–18.
- (7) Beskin, V. S.; Balogh, A.; Falanga, M.; Treumann, R. A. In *The Strongest Magnetic Fields in the Universe*; Springer New York: 2016, pp 3–14.
- (8) Olausen, S. A.; Kaspi, V. M. *The Astrophysical Journal Supplement Series* **2014**, 212, 6.
- (9) Braithwaite, J.; Spruit, H. C. *Astronomy & Astrophysics* **2006**, 450, 1097–1106.
- (10) Konar, S. *Journal of Astrophysics and Astronomy* **2017**, 38.
- (11) Konar, S. et al. *Journal of Astrophysics and Astronomy* **2016**, 37.
- (12) Konar, S.; Deka, U. *Journal of Astrophysics and Astronomy* **2019**, 40.
- (13) Sartore, N.; Ripamonti, E.; Treves, A.; Turolla, R. *Astronomy and Astrophysics* **2010**, 510, A23.
- (14) Kaspi, V. M. *Proceedings of the National Academy of Sciences* **2010**, 107, 7147–7152.
- (15) Mereghetti, S. In *High-Energy Emission from Pulsars and their Systems*; Springer Berlin Heidelberg: 2010, pp 345–363.
- (16) Weber, F.; Orsaria, M.; Rodrigues, H.; Yang, S.-H. *Proceedings of the International Astronomical Union* **2012**, 8, 61–66.
- (17) Lattimer, J. **2004**.
- (18) *Neutron Stars I*; Haensel, P., Potekhin, A. Y., Yakovlev, D. G., Eds.; Springer New York: 2007.
- (19) Bocquet, M.; Bonazzola, S.; Gourgoulhon, E.; Novak, J. ROTATING NEUTRON STAR MODELS WITH MAGNETIC FIELD, 1995.
- (20) Yuan, Y. F.; Zhang, J. L. *The Astrophysical Journal* **1999**, 525, 950–958.
- (21) Cardall, C. Y.; Prakash, M.; Lattimer, J. M. *The Astrophysical Journal* **2001**, 554, 322–339.

- (22) Mao, G.-J.; Iwamoto, A.; Li, Z.-X. *Chinese Journal of Astronomy and Astrophysics* **2003**, 3, 359–374.
- (23) Ryu, C. Y.; Cheoun, M.-K. *Journal of Physics: Conference Series* **2011**, 312, 042021.
- (24) Bordbar, G. H.; Rezaei, Z. *Research in Astronomy and Astrophysics* **2013**, 13, 197–206.
- (25) Bucciantini, N.; Pili, A. G.; Zanna, L. D. *Journal of Physics: Conference Series* **2016**, 719, 012004.
- (26) Chatterjee, D.; Elghozi, T.; Novak, J.; Oertel, M. *Monthly Notices of the Royal Astronomical Society* **2015**, 447, 3785–3796.
- (27) Bowers, R. L.; Liang, E. P. T. *The Astrophysical Journal* **1974**, 188, 657.
- (28) Chatterjee, D.; Novak, J.; Oertel, M. *Physical Review C* **2019**, 99.
- (29) Fiziev, P.; Marinov, K. *Astrophysics and Space Science* **2016**, 362.
- (30) Iserles, A., *A First Course in the Numerical Analysis of Differential Equations*; Cambridge University Press: 2008.